https://ntrs.nasa.gov/search.jsp?R=19680027186 2020-03-12T05:47:50+00:00Z

00018

HIGH-TEMPERATURE LM CATHODE ION THRUSTERS

N68-36658 (ACCESSION NUMBER) 42 (PAGES) CR 97210 (NASA CR OR TMX OR AD NUMBER) 1 (THRU) 08 (CODE) 03 (CATEGORY) FACILITY FORM 602

QUARTERLY PROGRESS REPORT NO. 2

5 MAY 1968 through 4 AUGUST 1968

CONTRACT JPL952131

by

J. HYMAN, JR., W. O. ECKHARDT,

AND J. A. SNYDER

15 AUGUST 1968

GPO PRICE $ _____

CSFTI PRICE(S) $ ___ ___

Hard copy (HC) ___ ___

Microfiche (MF) ___ ___

ff 653 July 65

OCT 1968 RECEIVED NASA STI FACILITY INPUT BRANCH

HUGHES

HUGHES AIRCRAFT COMPANY

RESEARCH LABORATORIES

MALIBU, CALIFORNIA

90265

"This report contains information prepared by the Hughes Research Laboratories under JPL subcontract. Its content is not necessarily endorsed by the Jet Propulsion Laboratory, California Institute of Technology, or the National Aeronautics and Space Administration".

HUGHES RESEARCH LABORATORIES
Malibu, California

a division of hughes aircraft company

HIGH-TEMPERATURE LM CATHODE ION THRUSTERS

Quarterly Progress Report No. 2
5 May 1968 through 4 August 1968
Contract No. JPL 952131

J. Hyman, Jr., W. O. Eckhardt,
and J. A. Snyder
Plasma Physics Department

15 August 1968

"This work was performed for the
Jet Propulsion Laboratory,
California Institute of Technology,
as sponsored by the
National Aeronautics and Space Administration
under Contract NAS 7-100
(Task Order #RD-26)."

PRECEDING PAGE BLANK NOT FILMED.

ABSTRACT

A 20-cm electron-bombardment thruster with a high-temperature LM cathode was operated with a beam current $I_B \approx 600$ mA at a specific impulse $I_{sp} = 6,200$ sec. Total source energy per ion $V_S = 260$ eV/ion was measured at a mass utilization efficiency $\eta_m = 80\%$. (V_S includes all power to form the ions, because no vaporizer, cathode heater, or keeper power is required with the LM cathode.) Operation at $I_{sp} = 4,400$ sec resulted in 50 eV/ion increase in discharge-chamber losses. Fabrication of a thermally integrated 30-cm thruster is essentially complete and assembly has begun. Satisfactory operation has been demonstrated with both annular and linear-slit cathodes which utilize a 2.5 μm tantalum shim to establish the narrow feed channel. The annular cathode operated satisfactorily in the 20-cm thruster at a temperature sufficiently high (200°C) to permit radiant cathode cooling. An LM cathode neutralizer in which the arc-spot pattern is always located on non-permanently-wettable material performed satisfactorily. Measurements of Poiseuille flow through a single-capillary flow impedance were linear and repeatable ($\pm$ 5%) over the range 1 A $< I_a <$ 5 A. Tests in the fractional ampere range are underway. LM cathode operation has been demonstrated under conditions of high-voltage isolation.

PRECEDING PAGE BLANK NOT FILMED.

TABLE OF CONTENTS

PRECEDING PAGE BLANK NOT FILMED.

LIST OF ILLUSTRATIONS

I. INTRODUCTION AND SUMMARY

A program of research and development is currently under way at the Hughes Research Laboratories to optimize LM cathode electron-bombardment thrusters. This program benefits extensively from recent experimental advances in thruster operation at HRL, JPL, and LeRC.

The design has been completed of a 30-cm electron-bombardment thruster in which the LM cathode is thermally integrated to the thruster. While operating at a temperature of 200°C-300°C the LM cathode can reject its own thermal load along a tapered aluminum backplate to the outer thruster shell where it is radiated to space at a shell temperature of 150°C. Since the design of the 30-cm thruster is based on the use of aluminum as a major structural material, the compatibility of aluminum with mercury in the thruster environment undergoes a continuing examination. We believe 6061 aluminum alloy to be compatible with this environment.

The ion-extraction system associated with the 30-cm thruster utilizes conventional state-of-the-art techniques for the design of high-perveance, drilled-plate electrodes.

Fabrication of both the ion-extraction electrodes and most of the component parts of the 30-cm thruster is complete, and assembly has begun.

A simple and workable technique has been established to assemble annular and linear-slit cathodes with a uniformly narrow feed-channel gap. After careful machining of the surfaces which form the opposing walls of the feed channel, they are mated together with only a narrow 2.5 μm tantalum shim separating them - no shim stock being placed in the gap which serves as the feed channel. An annular cathode fabricated with this technique has been operated in a diode discharge at both low temperature (20°C) and at high temperatures (200···300°C). The quantity of heat delivered by the discharge to the cathode under any of the conditions of high-temperature operation was sufficiently small to permit its radiant dissipation from the 30-cm thruster. The variation of the specific thermal load $V_{K,th}$ with cathode temperature and with neutral mercury flow rate is consistent with our analytical model of LM cathode operation.

The experimental linear-slit cathode fabricated with the tantalum shim technique and the experimental circular cathode fed by a single-capillary impedance have both been tested successfully at relatively low temperatures (up to 120°C). The circular cathode is not intended for high-

temperature, high-current use, and the linear-slit cathode will next be modified to permit high-temperature operation.

A new LM cathode neutralizer design has been conceived, implemented, and tested. It was aimed at combining the advantages of the bi-metal neutralizer structure (minimum variation of the arc-spot pattern diameter for a given feed-rate fluctuation) with those of the main thruster cathode (arc-spot pattern always located on non-permanently-wettable material, hence no consumption of structural material). This objective has been achieved at the small cost of a $\lesssim$ 5-V increase in diode discharge voltage, compared with the previous neutralizer design.

Efficient discharge-chamber performance has been demonstrated by the 20-cm thruster when modified to accept a high-temperature LM cathode, and also when operated with a high-perveance ion extraction system at low specific impulse. Some increase in discharge chamber losses was encountered in both of these modifications. It is believed that a part of these increased losses is associated with a shift of the discharge parameters from a point of optimum operation, and that reoptimization under the new conditions will eliminate this part of the discharge chamber losses.

Single-capillary flow impedances continue to show promise for the measurement and control of mercury flowrate in the range from 1-5 $A_{equiv.}$ Mercury was driven through a single-capillary flow impedance, joined to a circular LM cathode, at pressures from zero to 50 psig over a period of one week. The rate of flow of mercury through the capillary was a linear function of the applied pressure and was repeatable to within an experimental accuracy of $\pm$ 5% of the full scale reading for all pressures in excess of zero psig ($\doteq$14.7 psia). A new flow system has been assembled which will permit better controlled testing of single-capillary flow impedances at low pressures, and is expected to permit the measurement and control of mercury flow rates in the fractional ampere range.

A liquid-mercury high-voltage isolator was developed under NASA contract NAS 7-100 (Task Order #RD-26). To demonstrate its compatibility with LM cathode operation, the isolator was joined to the circular LM cathode with a single-capillary flow impedance. Discharge operation under conditions of high-voltage isolation was demonstrated for periods of several hours of uninterrupted automatic operation at voltages up to 4.5 kV. The LM cathode functioned normally when operated in this manner.

II. 30-cm THRUSTER

A. Introduction

At the end of the previous quarter of the current effort, a 30-cm thruster had been designed to serve as a test vehicle for LM cathodes and related systems being developed under this contract. This thruster design borrows heavily from geometrical criteria evolved in the recent thruster optimization of the NASA 15-cm SERT II thruster at LeRC,[1,2,3] and attempts to exploit the experience gained through the recent development of thrusters at HRL,[4] JPL,[5] and LeRC.[6]

Subsequent to close scrutiny of the existing design, a partial redesign was initiated which affected several of the component parts, though the overall thruster is changed only slightly. The major differences occur in the accel-electrode mounting tabs which were redesigned to be shorter and wider for added strength and stability. Also at this time, the cross-section of the screen and magnetic-collar pole pieces were scaled down from the previously chosen value of twice the SERT II cross-sectional dimensions to the same cross-sectional dimensions as used in SERT II.

The decision to return to the SERT II dimension was based on the belief that whatever is the effect of the shape of these pole pieces it is only significant in their close proximity. Close to these pole pieces the curvature of the magnetic field is not significantly effected by the thruster diameter, and so the cross-sectional dimensions of the pole pieces should not be a function of the thruster diameter so long as the thruster diameter is much larger than these dimensions.

The design described in the following pages is our first approximation. Experimental testing will be required to dictate the next steps necessary for optimization of this design.

B. Discharge-Chamber Design

Fabrication of the component parts for the 30-cm thruster is essentially complete, and assembly has begun. Figure 1 is an assembly drawing of this thruster. The anode diameter of 30 cm is twice the value used for the SERT II thruster. The magnetic distributor and cathode pole pieces are scaled up by the same factor, however the screen and magnetic-collar pole pieces have retained the SERT II cross-sectional dimensions. The separation between the anode and the thruster shell has been decreased from the SERT II dimension to permit a more compact overall design. The magnetic field can be provided either by 12 permanent bar magnets or by 12 bar electromagnets; the latter will be used to find the optimum magnetic field strength. The length of the thruster is 20 cm and the total weight was estimated to be approximately 6.2 kg. An itemization of each of the component weights (both estimated and actual, where available) is given in TABLE I.

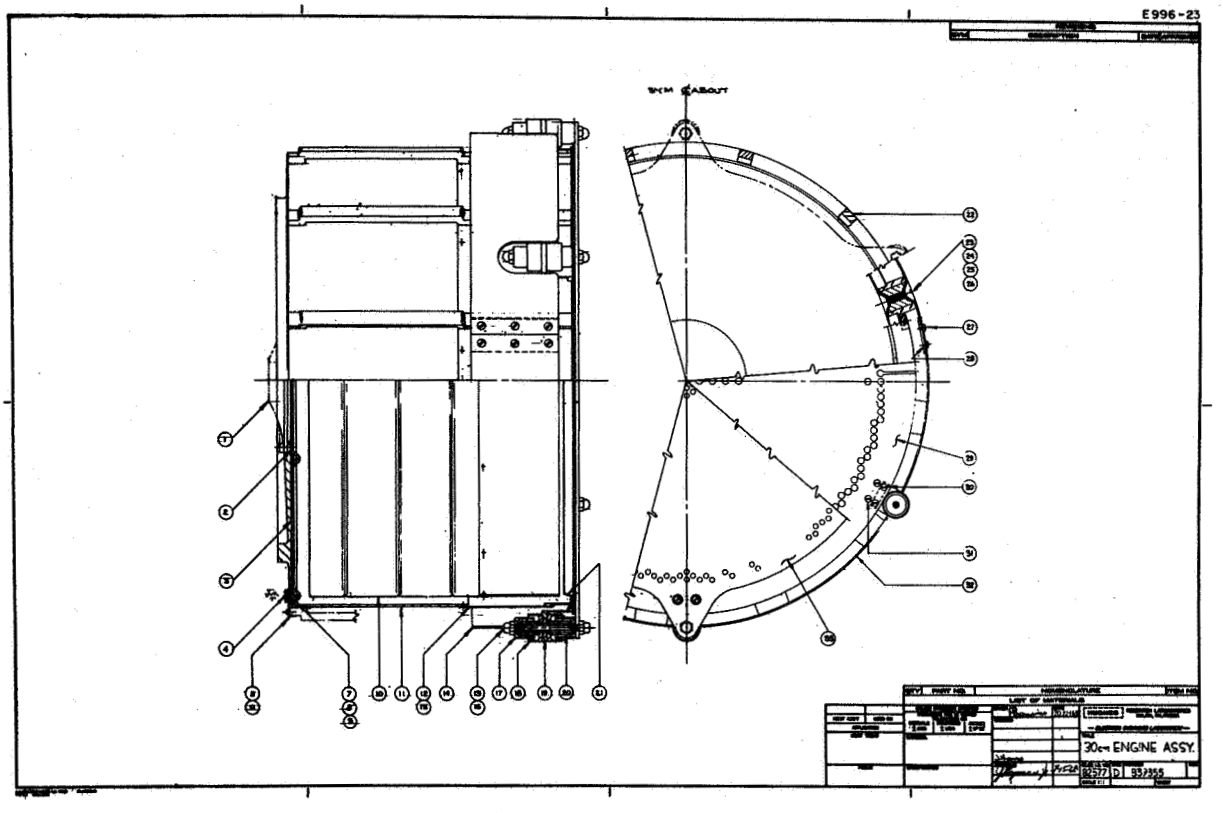

Fig. 1. Design of the 30-cm LM cathode thruster.

PART NO.	TITLE	No. Req.	CALCULATED UNIT WEIGHT kg	CALCULATED TOTAL WEIGHT kg	ACTUAL TOTAL WEIGHT kg
B-837977	Stud	6	.004	.024	.020
B-837982	Spacer	12	.003	.036	.021
D-839311	Screen elec.	1	.134	.314	(.314 est.)
D-839312	Accel elec.	1	.407	1.380	1.362
D-839313	Pole piece	1	.340	.340	.299
D-839314	Back plate	1	.660	.660	.650
D-839315	Anode	1	.145	.145	.149
C-839316	Rear anode	1	.220	.220	.257
C-839319	Lower housing	1	.710	.710	.532
C-839320	Upper housing	1	.130	.130	.133
B-839321	Bushing	12	.005	.060	.092
B-839322	Insulator	12	.014	.168	.158
D-839356	Anode connector	1	.160	.160	.166
C-839357	Splice	1	.007	.007	(.007 est.)
C-839358-99	Outer shield	12	.020	.240	.078
C-839358-98-1	Inner shield	6	.017	.102	.037
C-839358-98-3	Inner shield	6	.017	.102	.037
C-839359	Insul. support	6	.010	.060	(.060 est.)
C-839366-1	Aft pole piece	1	.270	.270	.181
C-839366-3	Aft pole piece	1	.285	.285	.183
C-839367	Pole piece back plate	1	.090	.090	.048
C-839368-98 -99	Mtg. nut, Mtg. screw } per set	12	.006	.072	(.072 est.)
C-839369	Magnet	12	.090	1.080	1.022
-------	Hardware, screws etc.	--	----	.074	.074
-------	Cathode plate	1	.134	.134	(.134 est.)
-------	LM cathode	1	.136	.136	(.136 est.)
TOTAL	30-cm THRUSTER	1	----	6.999	(6.222 est.)

TABLE I: Component weights for the 30-cm thruster.

The anode is attached to an external connector by a series of lead-throughs consisting of short aluminum rods which pass through insulating ceramic sleeves. These lead-throughs serve not only to connect the anode to the external electrical circuits, but also pass the discharge heat delivered to the anode on to the external connector. For a source energy per ion $V_S = 200$ eV/ion, the anode is expected to operate at an equilibrium temperature of 300°C for thrusters clustered in a peripheral array. Under these conditions, the cathode can operate also at a temperature of 300°C while rejecting its own thermal load along a tapered aluminum backplate to the outer thruster shell where it is radiated away at a temperature of 150°C. This calculation is based on demonstrated values of cathode performance given in Ref. 7, typically exhibiting a specific thermal load of $V_{K,th} = 7.5$ W/A for an LM cathode operating temperature of 300°C. In these calculations it was assumed that radiation is permitted only from the one exposed side wall of the thruster, and that there is no heat shielding between anode and cathode surfaces.

The design of the 30-cm thruster is based on the use of aluminum as the major structural material. This metal was chosen for the application because of its combination of light weight and high thermal conductivity, which together have resulted in the design of a light-weight thermally integrated thruster.

C. High-Perveance Ion-Extraction System

The design of the 30-cm ion-extraction system is based on information derived from various sources. In Ref. 8, Kramer and King report on an ion optical system suitable for extracting dense ion beams from gas discharges. Using the technique described by Hyman et al,[9] they studied the beam forming characteristics of their chosen geometries by using an automatic charged-particle trajectory tracer with space-charge simulation. These studies were confirmed by experimental measurements which showed that several of the ion extraction systems being studied operated satisfactorily over a wide range of mercury-ion beam current densities with accelerating voltages ranging from 3 to 7 kV. In the experimental studies the screen electrode hole diameter was 0.460 cm. Both cylindrical and countersunk screen holes were tested. The highest perveance was achieved with a pair of electrodes, separated by 0.250 cm, employing a countersunk screen electrode and an accel electrode having cylindrical holes of the same diameter.

More recently, Masek, Pawlik[5] have operated an ion-extraction system of similar hole size with a total accelerating voltage ranging from 3.2 to 4.6 kV. The nominal screen to accel spacing was 0.178 cm, though data are reported for spacings as small as 0.102 cm. Initially, a screen electrode thickness of 0.254 cm was used, but significant decreases in discharge chamber losses were realized by reducing the thickness to 0.076 cm. The 0.462 cm diameter holes in the screen were not countersunk. Accel electrodes were tested with hole diameters of 0.462 cm, 0.374 cm, and 0.318 cm, with a thickness of 0.254 cm. It was found that

accel impingement current increased only slightly in changing from an accel hole diameter of 0.462 cm to an accel hole diameter of 0.374 cm whereas discharge chamber efficiency improved by 20 eV/ion. Moreover, this slight increase in impingement current was more than offset by the increase in accel electrode mass, so that the overall electrode lifetime was expected to be a maximum at the 0.374 cm diameter.

In a related effort currently underway at HRL[10], variations of this same basic geometry are being analyzed in a detailed computer study. A screen electrode with countersunk holes of 0.475 cm diameter is paired with an accel electrode with a hole diameter of 0.360 cm. The design value of the interelectrode spacing, which is 0.228 cm, has been varied in order to analyze the effect of stress-induced perturbation of this spacing from the design value, as it may occur during thruster operation. In one variation the electrodes are separated by a distance of 0.178 cm, the nominal separation used in the JPL studies. At this separation, the particle flow remains essentially laminar (very little crossover) and all trajectories clear the accel electrode by a considerable margin. From this observation, it may be concluded that considerable leeway exists for the reduction of the interelectrode spacing before direct accel interception becomes a problem, a fact already demonstrated by the studies at JPL.

On the basis of all of the evidence given above, a basic design was chosen which is expected to yield high perveance (permitting maximum beam currents to be drawn at minimum accelerating potentials and therefore low specific impulse) as well as low interception (with the resultant long life expectancy). The basic design set is described by the following specifications:

Electrode	Material	Thickness	Hole Diameter	Distance Between Hole Centers	Hole Shape
Screen	Molybdenum	0.076 cm	0.475 cm	0.535 cm	Cylindrical
Accel	Molybdenum	0.254 cm	0.365 cm	0.535 cm	Cylindrical

To insure continuity of experiments with the 30-cm thruster, two complete sets of ion extraction electrodes are being fabricated at this time. Rather than making exact duplicates, opportunity was taken to test the effect on thruster performance of variations in hole size and shape. The additional electrodes ordered at this time are described below:

Electrode	Material	Thickness	Hole Diameter	Distance Between Hole Centers	Hole Shape
Screen	Molybdenum	0.076 cm	0.475 cm	0.535 cm	Countersunk
Accel	Aluminum	0.254 cm	0.475 cm	0.535 cm	Cylindrical
Accel	Molybdenum	0.254 cm	To be specified later	0.535 cm	To be specified later

The choice of aluminum for one of the accel electrodes was made to obtain an additional variation of ion-optics geometry at minimum cost, and is not meant to endorse aluminum as a suitable material for extraction electrodes in prolonged thruster operation.

The electrodes specified above can be operated in six possible combinations of hole size and shape:

1. 0.475-cm dia. accel with 0.475-cm dia. (cylindrical) screen
2. 0.475-cm dia. accel with 0.475-cm dia. (countersunk) screen
3. 0.365-cm dia. accel with 0.475-cm dia. (cylindrical) screen
4. 0.365-cm dia. accel with 0.475-cm dia. (countersunk) screen
5. Accel (to be specified) with 0.475-cm dia. (cylindrical) screen
6. Accel (to be specified) with 0.475-cm dia. (countersunk) screen.

D. Aluminum-Mercury Compatibility

From a survey of the available literature, it was previously concluded[4] that it appears reasonable to expect that a low-silicone alloy such as 6061 aluminum alloy can serve successfully as the major structural material in the fabrication of the 30-cm thruster. We have definite knowledge that this alloy has resisted attack by mercury droplets lying on the surface when the metal is exposed to normal atmospheric conditions, and there is reason to believe that it can also resist attack under the thruster operating environment of 475-675 K at a mercury vapor pressure of 10^{-4} Torr. The decision to fabricate the thruster from this alloy must be considered as an experiment, which will be of significant value in itself since it will answer a question of general importance for the development of electron-bombardment thrusters. While this choice has been made, research on the compatibility of aluminum alloys with the thruster environment continues.

To collect information relating to the compatibility of aluminum with mercury in the thruster environment, we have attached seven metallurgical samples to the anode of the 20-cm PMT. For purposes of comparison, both aluminum and non-aluminum samples are included in the following list of specimens:

1. Titanium
2. Nickel
3. 6061 aluminum alloy
4. Pure aluminum
5. Pure aluminum (sandblasted)
6. Molybdenum
7. Type 304 stainless steel

These samples are being left in place on the anode while the thruster is operating during the normal course of the thruster optimization program, and will be inspected from time to time for signs of deterioration. The first inspection, after 85 hours of thruster operation, showed no evidence of deterioration.

A recent experience at HRL has strengthened the conviction that alloys of aluminum are compatible with a mercury environment both at high and low temperatures. A 10-inch diameter high-vacuum pump station was recently disassembled for conversion from an oil to a mercury diffusion pump. Since this station had been operated for a number of years with experiments involving mercury, condensation of mercury had occured on many components of the station.

A considerable quantity of mercury lay in the aluminum housing of the high-vacuum gate valve. This housing was cast from A-356 aluminum alloy, which is relatively high in silicon: A-356 contains 7% silicon as opposed to 6061 with 0.6%. At first inspection there was no sign of corrosion even though the mercury had undoubtedly been in contact with the aluminum for many years. Within a few minutes, however, a white substance began to grow and protrude in bunches of parallel fibers perpendicular to the aluminum surface. Within an hour, growth of these fibers appeared to have stopped, however the growth of new bunches could be stimulated by scraping the mercury-covered aluminum surface. From this experience we again concluded that cold aluminum even of high silicon content is compatible with liquid mercury in the thruster vacuum environment, and that it suffers only tolerable attack when exposed to air.*

The oil diffusion pump also contained a considerable quantity of mercury. Since mercury has a much higher vapor pressure than diffusion pump oil at the operating temperature of 230°C, it is expected that during operation the liquid mercury is quickly vaporized and recondenses on colder surfaces of the vacuum system. Still, during the warm-up time

---

* Similar deposits have been observed previously at LeRC after extensive duration testing in which aluminum foils were used for erosion protection of flexible lines filled with liquid nitrogen. Analysis at that time indicated that the white substance was a hydrated aluminum amalgam. [11]

and whenever drops of mercury fall into the pump oil, the surfaces of the diffusion pump are subjected to the presence of mercury vapor. Though the vapor deflection vanes of the diffusion pump (which operate at the oil temperature of 230°C) were constructed entirely of aluminum, no attack of their surface was evident either at first inspection or thereafter.

III. LM CATHODE RESEARCH AND DEVELOPMENT

A. Introduction

In the First Quarterly Report[4] under the current effort it was stated that all previous annular cathodes had been fabricated with feed-channel gaps which were no smaller than 5 μm, and in many cases were larger. As a consequence, the required electron-to-atom ratios could only be obtained at high temperature by operating these cathodes in a mode which differs from that employed at low temperatures. The mode change is indicated by the observation that the specific thermal loading of the cathode, $V_{K,th} = P_{K,th}/I_K$, is not constant as the cathode temperature T_K is increased. Values for $V_{K,th}$ have been measured at 2.5 WA^{-1} for $T_K = 130^{\circ}C$, and up to 12 WA^{-1} for $T_K = 300^{\circ}C$. This change is due to the withdrawal of the exposed mercury surface (and hence the arc spots) into the annular channel at higher temperatures. This mode of operation is referred to below as the retracted-spot mode.

To avoid the necessity of operating in the retracted-spot mode, two new cathodes were constructed during the first quarter of the current effort; an annular cathode designated K-25-V, and a linear-slit cathode designated K-45. With both cathodes a common technique is employed to establish a uniformly narrow feed channel. In both cases, the two surfaces which form the opposing walls of the feed channel are first machined separately to very close tolerances. The two surfaces can then be lapped together (for the linear-slit cathode, the surfaces are flat and can be finished separately) to a perfect match. Then, the required annular feed channel separation is established by mating the two opposing surfaces together with a 2.5 μm thick tantalum shim separating them, no shim stock being placed in the gap which serves as the feed channel.

During the present quarter the linear-slit cathode K-45, the circular cathode K-41 (fed by a single-capillary impedance), and a new neutralizer cathode K-48 were operated in diode discharges, while the annular cathode K-25-V has been tested at high temperature both in a diode discharge and in actual thruster operation. The data obtained from the high-temperature tests substantiate the explanation given above for the dependence of $V_{K,th}$ on T_K.

B. Annular Cathode Operation

The annular cathode K-25-V was operated in a diode discharge at high temperature. The specific thermal load $V_{K,th}$ was measured at cathode body temperatures $T_K = 200^{\circ}C$, $250^{\circ}C$, and $300^{\circ}C$ as a function of the electron-to-atom ratio K_e/K_a. The data are plotted in Figure 2. The cathode ran stably at all temperatures, operating all day without spontaneous extinctions. The variations of $V_{K,th}$ were in accord with expectations based on our analytical model of the behavior of the arc spots.[7]

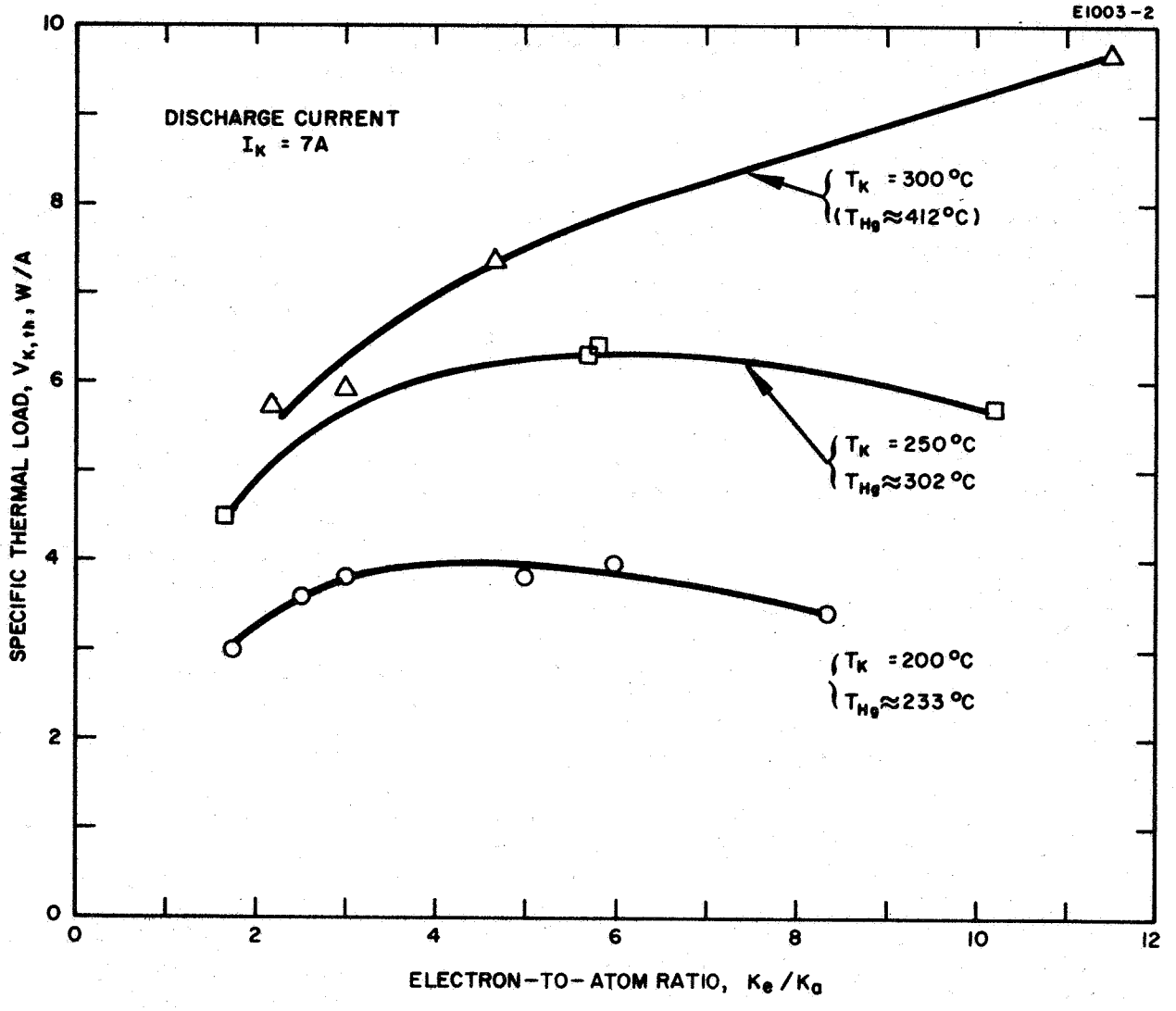

Fig. 2. Dependence of the specific thermal load ($V_{K,th}$) on cathode temperature (T_K) for LM cathode K-25-V.

At constant discharge current, either an increase in cathode temperature or a decrease in the mercury feed rate resulted in a shrinking of the exposed annular mercury surface. The width of the arc-spot pattern was observed to decrease with the mercury surface; and in the extreme limit, both the liquid surface and the arc spots receded into the 2.5 μm thick feed channel as the discharge shifted to the retracted-spot mode. This mode is characterized by an increase in $V_{K,th}$, the thermal power delivered to the cathode per unit discharge current.

The cathode was operated at high temperature over a period of several days in the range of interest for the 30-cm thruster which is currently being assembled. Anticipating operation at a beam current I_B = 1A, mass utilization efficiency η_m = 90%, discharge voltage V_D = 35V, and a source energy per ion of V_S = 250 eV/ion, the cathode was operated with a discharge current I_K = 7A and a neutral mercury flow rate I_a = 1.11A. At a cathode body temperature T_K = 200°C a specific thermal load $V_{K,th}$ = 3.8 W/A was measured. By calculating the temperature drop required to drive the heat from the mercury surface to the thermocouple location at a radius of 0.44 cm, we estimate that under the above conditions the mercury surface temperature was $T_{Hg} \approx 233°C$. At a calculated mercury surface temperature $T_{Hg} \approx 302°C$ (corresponding to a measured T_K = 250°C) the specific thermal load was $V_{K,th}$ = 6 W/A, and at a surface temperature $T_{Hg} \approx 412°C$ (T_K = 300°C) the specific thermal load was $V_{K,th}$ = 8 W/A. The heat delivered to the cathode under any of these three operating conditions can be accommodated by the thermal design of the 30-cm thruster.

The same annular cathode was also evaluated at high temperature in a diode discharge over a range of current suitable for operation in a 20-cm electron-bombardment thruster. Anticipating a beam current I_B = 600 mA, mass utilization efficiency η_m = 90%, discharge voltage V_D = 35 V, and a source energy per ion V_S = 280 eV/ion, we must operate at a discharge current I_K = 5 A and a neutral mercury flowrate I_a = 666 mA. As in the measurements in the range of interest for the 30-cm thruster, at a cathode body temperature T_K = 200°C (corresponding to $T_{Hg} \approx 224°C$ for I_K = 5A), a specific thermal load $V_{K,th}$ = 3.8 W/A was measured. Similarly, at T_K = 250°C (corresponding to $T_{Hg} \approx 326°C$) the specific thermal load was $V_{K,th}$ = 7 W/A. The quantity of heat delivered to the cathode under either of these conditions is sufficiently small to permit radiant dissipation from either the 30-cm thruster or from a similarly designed thruster of 20-cm diameter.

The fact that the two lower-temperature curves in Fig. 2 show a maximum of $V_{K,th}$ at $K_e/K_a \approx 4 \ldots 6$ is caused by operation with arc-spot patterns covering only part of the circumference of the cathode annulus. When the cathode is operated at electron-to-atom ratios above 4...6 (at the particular current of 7 A) a larger fraction of the circumference becomes utilized and $V_{K,th}$ decreases. Past experiments have shown that when a full-circle spot pattern is established, a minimum is reached beyond which $V_{K,th}$ rises monotonically. The K_e/K_a-range of Figure 2 is limited to the present range of interest for bombardment thruster cathodes. The T_K = 300°C curve does not show a maximum because at this temperature the spot pattern was always a full circle within this range.

C. Linear-Slit Cathode Operation

The linear-slit cathode shown schematically in Fig. 3 was assembled with a uniformly narrow feed channel separation established by inserting a 2.5 μm thick tantalum shim between the walls on either side of the pool-keeping structure which is formed by pressing together the two cathode halves. The cathode halves were held together in an experimental mounting clamp which also contains a porous tungsten flow impedance, flow channels, seals etc. The cathode assembly was operated in a diode discharge, and the formation of the expected linear arc-spot pattern was observed. There was, however, a pronounced tendency of the spot pattern to attach itself preferentially to the narrow side surfaces of the tantalum shims which form part of the surface of the pool-keeping structure. Nevertheless, encouraging performance was obtained at temperatures $T_K = 80^oC$ (20 electrons per atom at $I_K = 10$ A) and $T_K = 120^oC$ (12 electrons per atom at $I_K = 6A$). The seals used in the assembly will now be changed to permit operation at higher temperatures.

In view of the present encouraging performance of the annular design, the need for development of the linear-slit cathode is considerably diminished. One of the benefits initially conceived to be applicable only with the linear-slit design (the use of the tantalum shim to establish a uniformly narrow feed gap) has also been reaped by its adoption into the design of an annular cathode. Still, the simplicity of maintaining close tolerances in the linear-slit configuration cannot be matched by any other geometry which is suitable for high-current, high-temperature designs. Therefore, the linear-slit cathode remains a candidate for future investigation under the present contract.

D. Circular Cathode with Single-Capillary Impedance

The experimental LM cathode with its associated single-capillary flow impedance (as described in the First Quarterly Report)[4] was operated in a diode discharge. The cathode operated in a satisfactory manner at currents up to 25 A. In this initial diode test, the cathode was water cooled to 20^oC. The cathode has since been equipped with a heat exchanger which will permit high-temperature operation. Under this condition, the exposed mercury surface of the pool-keeping structure will become sufficiently small to permit visual observation of the magnitude of mercury flow fluctuations. The geometry of this combination of cathode and flow impedance is expected to offer a decrease in the amplitude of such fluctuations.

As was explained in the First Quarterly Report[4], the design of this cathode-impedance combination should lead to an increased measure of stability of the mercury surface position which had previously been achieved only by the use of a permanently wettable metal to stabilize the position of the liquid metal surface. This stability can be expected to occur only if the single-capillary impedance is free of gas or vapor bubbles and has an absence of obstructions or constrictions. Particularly in the low-flow portion of their usable range, certain ambiguities exist so far in the per-

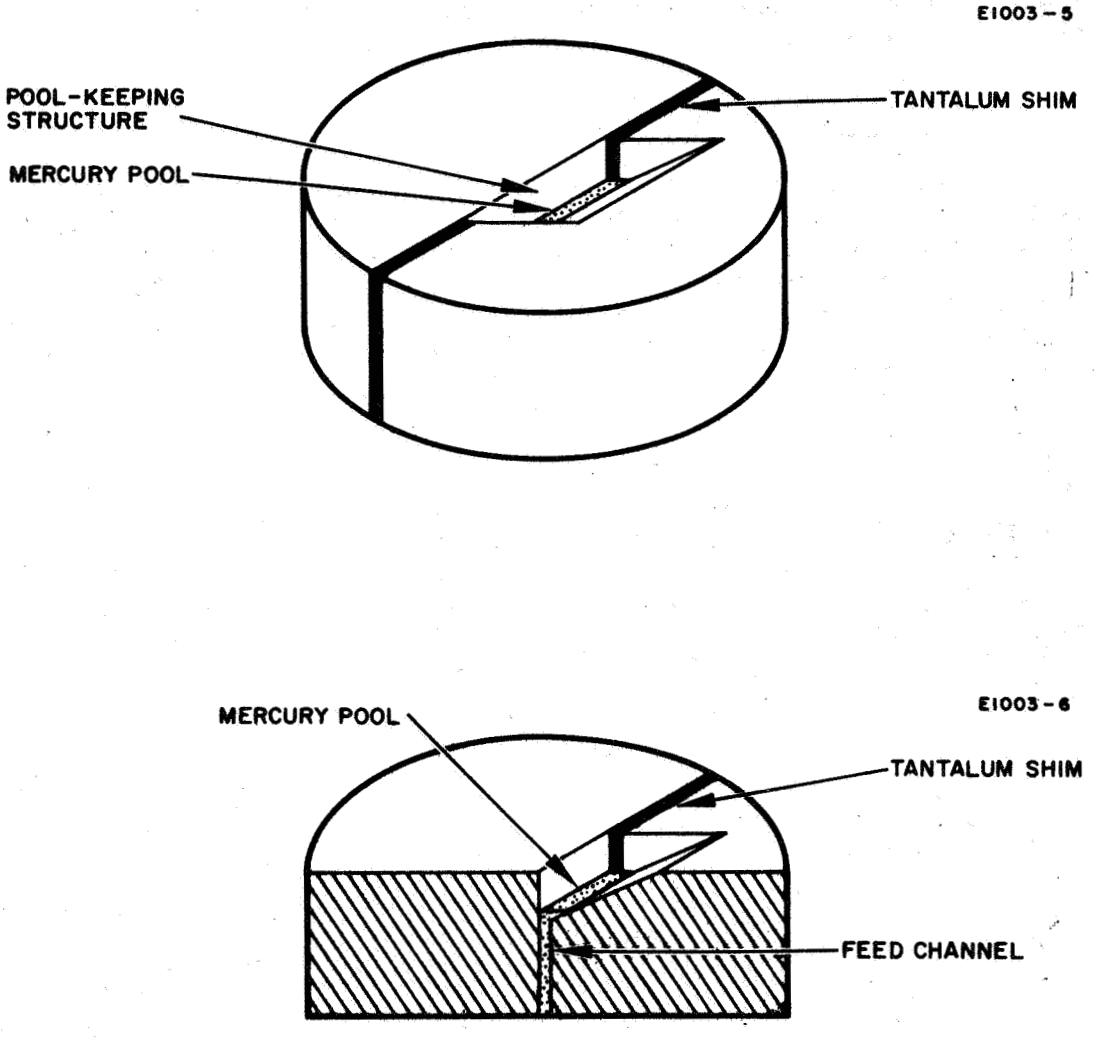

Fig. 3. Schematic drawing of experimental linear-slit LM cathode K-45

formance of single-capillary impedances; this may indicate that the stated requirements are not being met.

Experiments which are described in Section V-A are currently underway to resolve the ambiguity before this cathode-impedance combination is subjected to further diode testing.

E. LM Cathode Neutralizer

During this reporting period a new LM cathode neutralizer design has been conceived, implemented, and tested. It was aimed at combining the advantages of the bi-metal neutralizer structure (minimum variation of the arc-spot pattern diameter for a given feed-rate fluctuation) with those of the main thruster cathode (arc-spot pattern always located on non-permanently-wettable material, hence no consumption of structural material). This objective has been achieved at the small cost of a $\lesssim$ 5-V increase in diode discharge voltage, compared with the previous neutralizer design.

The new neutralizer has been operated for periods of several hours at currents within the beam current range of a 30-cm thruster, and good stability (e.g., an average of 1.5 spontaneous extinctions per hour, automatically reignited by a stationary pulse igniter) has been demonstrated. Typical data points which were obtained without trying to maximize the electron-to-atom ratio (K_e/K_a) are as follows:

Neutralizer Current, A	Discharge Voltage, V	K_e/K_a	Run Duration, hours
2.5	25.5	95	1.1
1.82	25	67	3.5
1.06	24.5	43	5.3
1.05	24	45	6.7
0.78	25	33	2
0.5	22.5	20	4.5

The experimental arrangement has since been modified to permit the use of the igniter electrode as a probe for measuring the floating potential in the vapor jet of the neutralizer cathode, and an attempt has been started to correlate this potential with the electron-to-atom ratio, in order to be able to control the neutralizer feed rate on the basis of a continuous monitoring of this potential. Preliminary data, taken at a substantially constant flow rate and variable current, show that such a correlation may indeed exist. More data, especially at variable flow rate and constant current, are required however before a conclusion on the suitability of this method can be drawn.

IV. LM CATHODE THRUSTER OPERATION

A. Introduction

Thruster operation during the first quarter of the current effort was directed at improving the discharge chamber performance of a 20-cm bar-electromagnet thruster. An existing thruster was modified to conform (in first approximation) to the magnetic field geometry of the LeRC 15-cm SERT II thruster. It was equipped with a magnetic collar and with both screen and cathode pole pieces to reproduce the desired magnetic field profile. A baffle was placed downstream of the cathode pole piece. The exact configuration was modified in a series of separate experiments. By the end of the first quarter, discharge chamber losses had been reduced to a total V_S = 235 eV/ion* at a mass utilization efficiency η_m = 80%.

During the current quarter no effort has been expended to further optimize the thruster. Rather, the emphasis has been concentrated on demonstrating similar discharge chamber performance when the thruster was modified to accept a high-temperature LM cathode, and also when it was operated with a high-perveance ion-extraction system.

In essence both goals have been accomplished, though some increases in discharge chamber losses have been encountered with both of these modifications. It is believed that most of the increases are associated with a shift of the discharge parameters from the point of optimum operation, rather than any inherent effects associated with either modification per se.

B. Operation with a High-Temperature LM Cathode

As a first step in the thermal integration of an LM cathode with an electron-bombardment thruster, LM cathode K-25-V was operated in the 20-cm thruster at a cathode body temperature T_K = 200°C (depending on the discharge current I_K, the mercury surface temperature T_{Hg} is somewhat higher.) This temperature is sufficiently high to permit radiant dissipation of discharge heat from a thermally integrated electron-bombardment thruster whether it be the 30-cm thruster presently being fabricated or from a similarly designed 20-cm thruster. Complete thermal integration will be demonstrated with the 30-cm thruster; with the existing 20-cm thruster this cannot be done conveniently, because the LM cathode assembly is not thermally coupled to the outer surfaces of the thruster from which the heat would be radiated.

---

* V_S, the total source energy per ion, is equal to the discharge energy per ion, because no heater, vaporizer, or keeper power is required with the LM cathode.

At $T_K = 200^oC$ the inherent LM cathode losses $V_{K,th}$ are nearly the same as are encountered at lower temperatures. Accordingly, there is no reason a priori to expect the discharge-chamber performance to vary significantly depending on whether the electrons are generated by a low-temperature or by a high-temperature LM cathode. Because of the physical size of the existing heat sink attached to the high-temperature cathode, it was not convenient to mount the cathode at the same position as had been employed with the movable low-temperature LM cathode (shown in Fig. 11 of Ref. 4). At that time a cathode recess 1 cm $< \ell <$ 3 cm was found to result in minimum discharge chamber losses. As shown in Fig. 4, cathode K-25-V was mounted at $\ell = 5$ cm, a full 2 cm upstream of the optimum region. Nevertheless, discharge-chamber losses remained relatively low.

The discharge-chamber performance of this configuration is shown in Fig. 5. The lower performance curve (marked 6 kV) can be compared with the performance curve representing the optimum configuration tested with the movable low-temperature cathode (Fig. 13 of Ref. 4). In general a penalty of 20-40 eV/ion has been paid for the convenience of placing the LM cathode totally outside of the cathode pole piece. From this comparison it is concluded that no significant degradation occurs in discharge chamber performance in response to the transition from a low-temperature to a high-temperature LM cathode. In any more permanent construction, such as the 30-cm thruster, the high-temperature LM cathode would of course be placed at whatever position results in optimum performance.

C. Operation at Low Specific Impulse

An interaction exists between discharge-chamber performance and the conditions of ion extraction. Langmuir probe measurements of the plasma near the axis of the 20-cm solenoid-magnet LM cathode thruster have shown that the plasma electron temperature shifts from $T_e = 6.2$ eV when the discharge-chamber is operating without beam extraction to a value of $T_e = 11.3$ eV when a beam is being extracted. Furthermore, the discharge-chamber efficiency in an LM cathode thruster is known to respond to variations in the conditions of extraction[12]. In Ref. 12 discharge chamber losses were reported to increase by 20 eV/ion at $\eta_m \approx 85\%$ when the beam was extracted at a specific impulse $I_{sp} = 3,360$ sec, rather than at $I_{sp} = 6,700$ sec.

One mechanism by which the characteristics of the discharge are known to be coupled to changes in the accelerating voltage of the ion-extraction system is through a shifting in the equilibrium position of the beam-plasma interface. At constant beam current, this interface shifts in response to changes in the total accelerating voltage. This interaction was elaborated on in some detail by Hyman et al,[9] who demonstrated that the interface between the ion beam and the plasma recedes upstream into the discharge chamber as the ion-extraction perveance is decreased. For a given ion-extraction system at fixed beam current, the perveance decreases as the total accelerating potential is increased and increases as

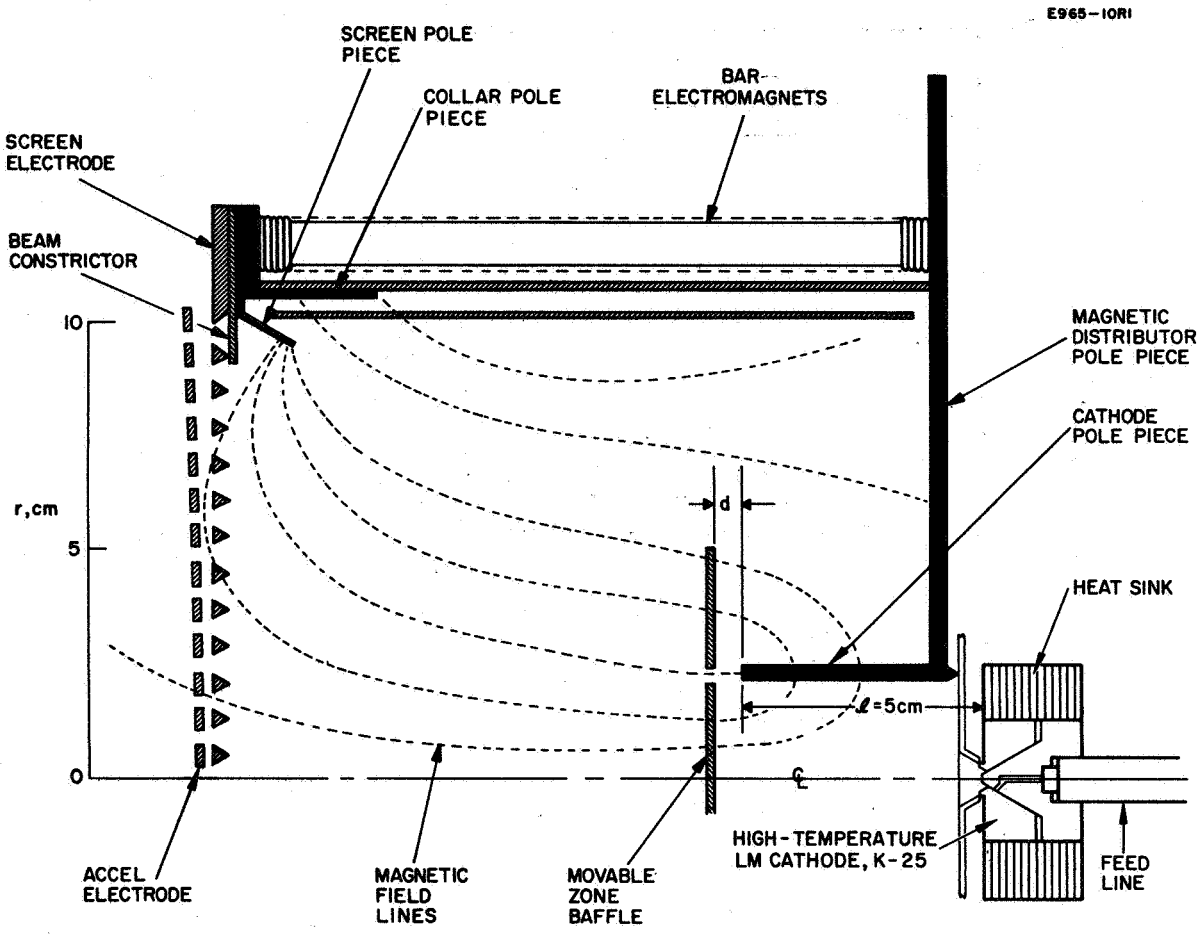

Fig. 4. Schematic drawing of the 20-cm bar-electromagnet thruster with a high-temperature LM cathode.

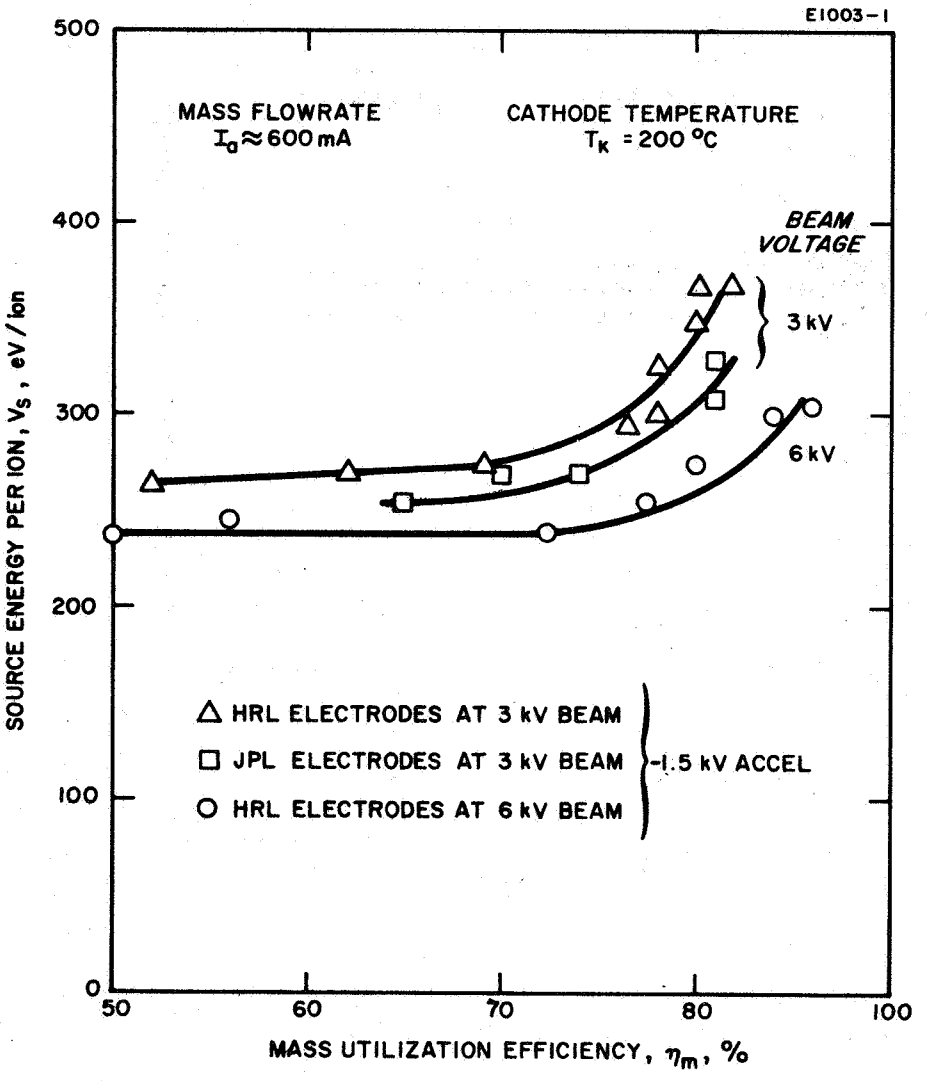

Fig. 5. Effect of extraction potential on discharge-chamber performance of the 20-cm bar-electromagnet thruster with a high temperature LM cathode.

the total accelerating potential is decreased; so that a fixed ion-extraction system can operate at any of various values of operating perveance. So long as the accel interception current remains sufficiently low there is no inherent advantage, insofar as the dynamics of ion extraction are concerned, to operating at one perveance or another. A discharge chamber which has been set up to operate at maximum efficiency with a given total accelerating voltage may, however, shift from this optimum condition in reaction to shifts in the position of the plasma interface which occur when the total accelerating potential is varied.

The 20-cm thruster with high-temperature LM cathode K-25-V was operated at beam voltages of 6 kV and 3 kV. In either case the accel electrode was biased at 1.5 kV and the accel interception current was typically 1/2% of the beam current. With this thruster, variations in the total accelerating potential had a pronounced effect on discharge-chamber performance.

In Fig. 5 the upper and lower performance curves were obtained with an HRL ion-extraction system* similar to the one used for the 4,000-hr life test of an LM cathode electron-bombardment ion thruster which was completed in 1966. The lower curve was obtained at a beam voltage of 6 kV (which was used throughout the recent discharge-chamber optimization program) and the upper curve was obtained with the same ion-extraction system operated with a beam voltage of 3 kV. At a mass utilization efficiency η_m = 80% the required source energy per ion is increased by 100 eV/ion by operating at the lower beam voltage (the total accelerating voltage being lowered accordingly from 7.5 kV to 4.5 kV).

A second set of 20-cm diameter electrodes of an entirely different design** are presently on loan to HRL from JPL. Using the JPL ion-extraction system with the 20-cm HRL thruster, an ion-beam was extracted at a beam voltage of 3 kV as had previously been done with the HRL system. At a mass utilization efficiency of 80% the discharge-chamber losses were reduced by 30 eV/ion from the value observed at the same voltage with the HRL system.

---

* In this system the apertures in the screen electrode are countersunk on the plasma side. The center spacing between screen electrode and accel electrode is 0.150 cm, and the electrode spacing at the anode radius is 0.235 cm. The closer spacing in the center provides a quasi-matching of perveance density and current density. The hole pattern has a hexagonal close-packed array of 1027 holes with a nominal diameter of 0.476 cm and a hole center spacing of 0.635 cm, drilled in 0.158 cm thick molybdenum plates. The open area is 51%.

** This ion extraction system is similar to one used in recent studies conducted at JPL related to thrust system technology for solar-electric propulsion.[5] The apertures of the screen electrode of this system are not countersunk and the hole diameter in both the screen and accel is 0.462 cm. The screen thickness is 0.076 cm, and the accel electrode is 0.254 cm thick. The open area is about 75%. For the data shown in Fig. 5 the interelectrode spacing was set at 0.076 cm.

Neither the degraded performance obtained at 3 kV with the HRL system, nor the extent to which performance was regained by using the JPL system, are meant to demonstrate any ultimate limitation associated with either system or in fact with the HRL 20-cm thruster. All that has been demonstrated is that variations in conditions of ion-beam extraction do result in variations in discharge-chamber performance, and that to the extent that these variations shift the discharge parameters away from an optimum condition these variations can result in significant increases in discharge losses. It is believed that these losses can again be reduced by re-optimization of the discharge chamber at any chosen beam-extraction voltage. The 20-cm thruster was originally optimized for a specific impulse $I_{sp} \approx 6000$ sec to permit comparison of thruster performance with that obtained earlier.[7,12] Current mission analyses directed at solar-electric missions indicate that lower values of specific impulse are desirable for these missions.[13] Accordingly, further optimization of the 20-cm thruster and the forthcoming optimization of the 30-cm thruster will be attempted at lower values of beam voltage.

V. FLOW SYSTEMS

A. Single-Capillary Flow Measurements

1. -Cathode feed system

During this quarter the single-capillary flow impedance SC-2 associated with cathode K-41 was evaluated both with and without the cathode attached. This device, shown schematically in Fig. 6, consists of 150 cm of 0.0112 cm i.d. tubing wound about a spool and then totally enclosed by a standard 3/8 in. diameter mercury feed and vacuum lead-through tube. Both the upstream and downstream ends of the capillary are attached to the feed tube with a nickel-titanium eutectic braze. Similar to the results previously reported with capillary SC-1, the rate of flow through this impedance was linear and repeatable over a period of one week to within the experimental accuracy of + 5% of the full-scale reading for all pressures in excess of zero psig (= 14.7 psia). As in previous single-capillary tests, greater scatter of the data points was apparent at 14.7 psia.

Data plotted in Fig. 7 relate the mercury flowrate (expressed in equivalent amperes) to the driving pressure across the impedance alone in one case, and across the impedance with the cathode attached in the other. The incremental increase in flow with driving pressure is the same in either case: $I_a/p = 0.08$ A/psi.

Within experimental error, the measured flow impedance is identical to the predicted value based on the best known dimensions of the stainless-steel capillary tubing. Though the original design called for a single-capillary tube of 250 cm length, the final assembly was completed with a 150 cm capillary; the capillary as received from the manufacturer was shorter than had been requested, and further shortening occurred during fabrication. By examining several tube cross-sections taken from the end of the capillary, the inner diameter of the capillary was found to be 0.0112 cm.

Though the flowrate at a given pressure changes when the cathode is attached to the capillary, the incremental rate of rise does not change. The attachment of the cathode does not significantly increase the impedance, but rather introduces a constant pressure increment. The source of this pressure increment is related to the minute flow fluctuations which were predicted earlier to occur in the region of minimum constriction of the cathode feed channel.[4]

The reasons for the fluctuations in the feed channel have previously been described as follows:

> Let us assume that a steady mercury flow is provided at the entrance of the minimum-diameter section of the feed channel shown in Fig. 8. The mercury passes through the feed

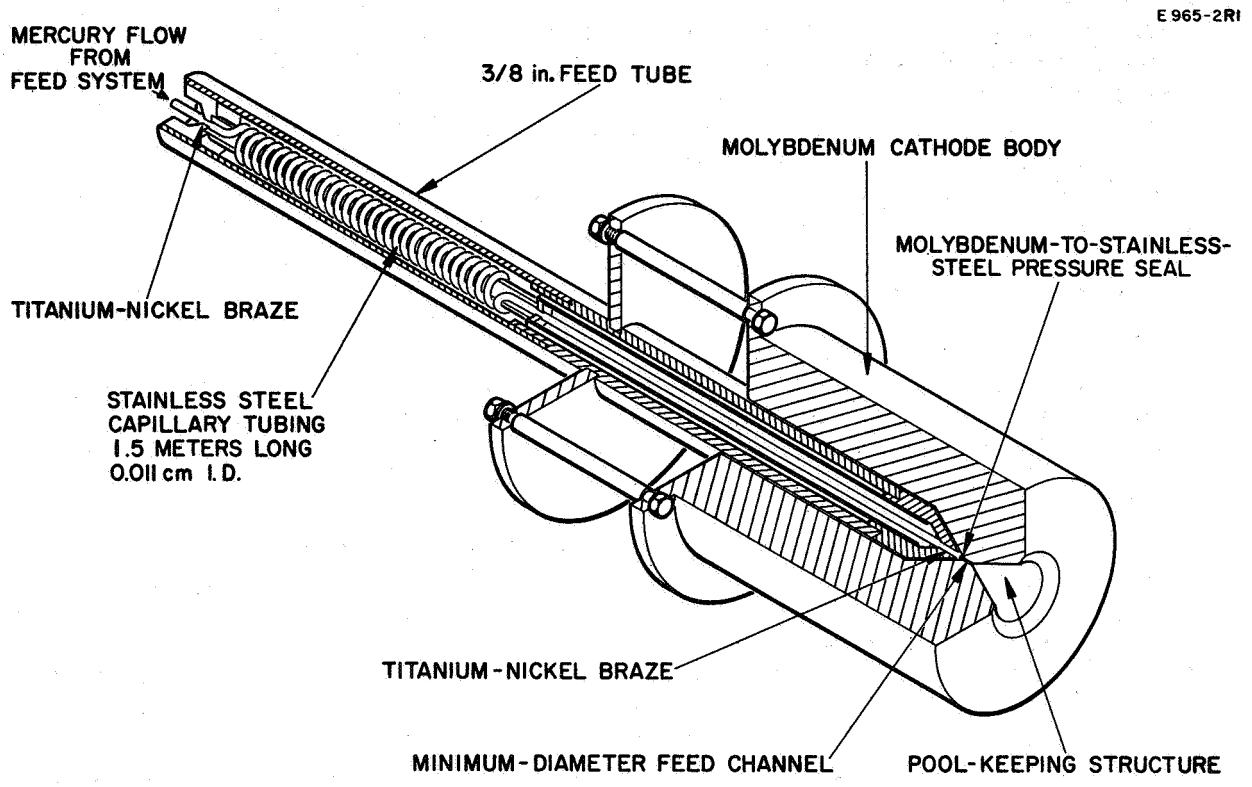

Fig. 6. Circular cathode K-41 with single-capillary flow impedance SC-2.

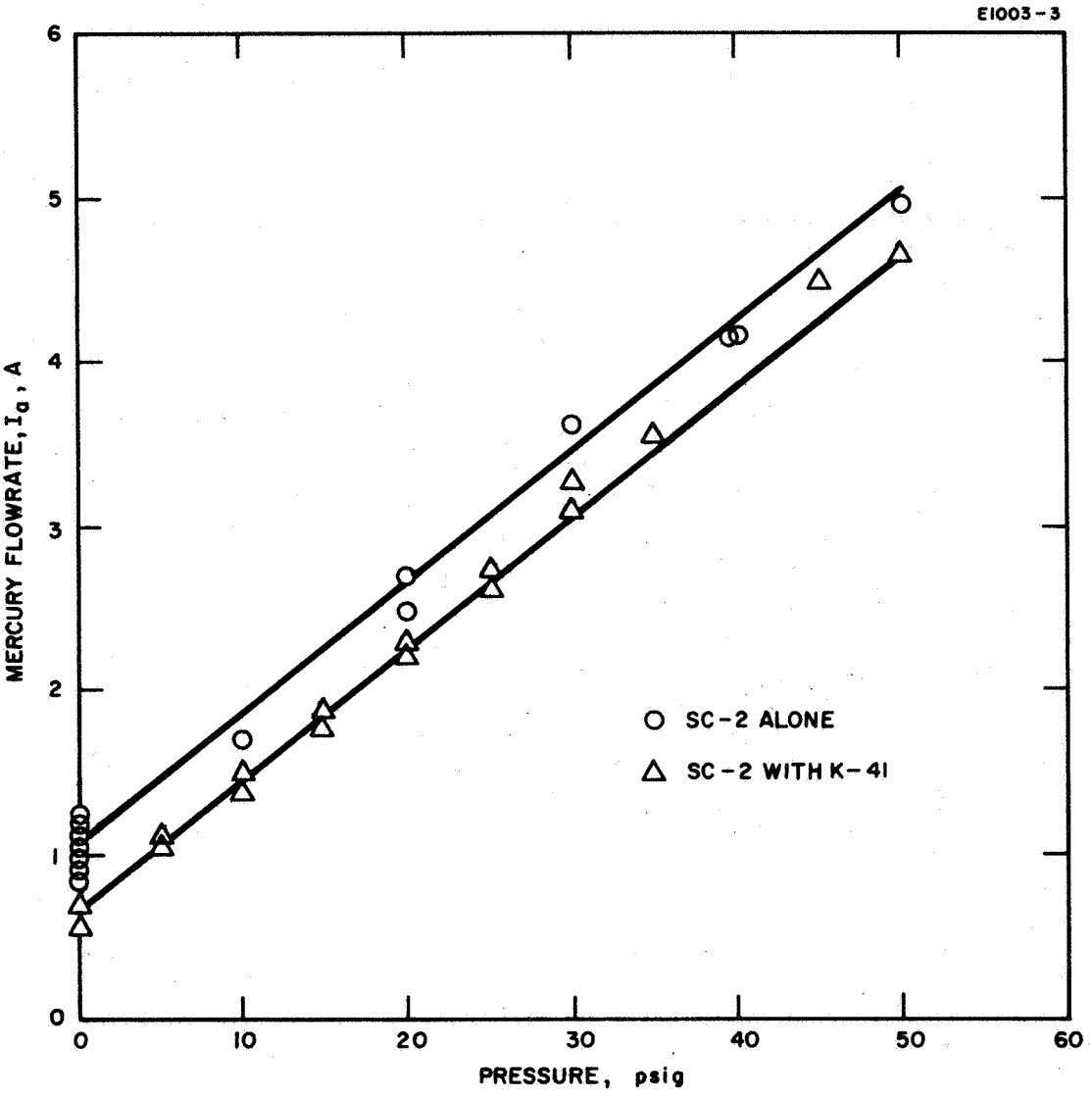

Fig. 7. Impedance characteristics of single-capillary impedance SC-2, showing the effect of attaching LM cathode K-41.

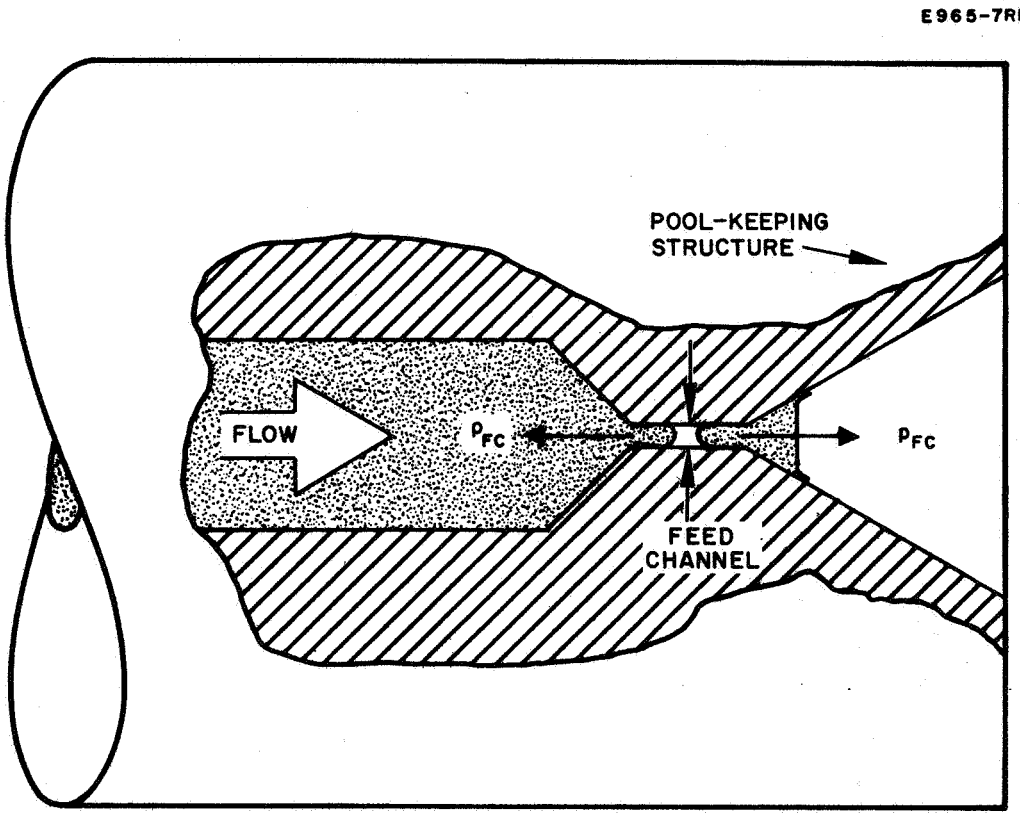

Fig. 8. Pressure increment p_{FC} due to surface-tension forces.

channel and into the pool-keeping structure. The liquid in the pool-keeping structure is at a very low pressure determined by surface-tension forces, by the momentum change imparted by surface evaporation of mercury atoms, and by arc pressure. Since the pressure exerted by surface tension is inversely proportional to the radius of curvature of the liquid surface,* the magnitude of the pressure due to surface tension rises greatly to a value p_{FC} within the feed channel where the radius of curvature is a minimum (the radius of curvature being equal to that of the feed channel). In the upstream direction, the pressure p_{FC} is balanced by the driving pressure of the flow system. In the downstream direction, however, p_{FC} may not be balanced and thus the downstream segment of the minimum-diameter mercury column is unstable and tends to be expelled into the pool-keeping structure. Such expulsion leaves a void, and no further mercury flow enters the pool-keeping structure until the void is filled by flow from the source, at which moment the system is again unstable and the mercury contained in the feed channel may again be expelled into the pool-keeping structure.

Since such a void exists in general within the feed channel (which is part of the cathode), a pressure p_{FC} is generated opposing the driving pressure, when the cathode is attached to the single-capillary flow impedance. This back pressure must be canceled by an equal driving pressure increment to maintain a given flow rate through the single-capillary flow impedance when the cathode is attached. The experimentally measured pressure increment of 5 psi is consistent with the value calculated in accordance with this model.

2. Research on single-capillary flow

The cause of increased scatter of the data points in the vicinity of 14.7 psia in recent single-capillary flow measurements is not presently understood. Such scatter has been reported previously[4] in the testing of capillary SC-1 where this and other unexplained phenomena were observed. In these experiments, excursions beyond the normal operating range (20-75 psia) resulted in certain systematic variations in the flow rate. Zero flow was observed for driving pressures of less than 10 psia, and the flow was substantially reduced for a period of about 30 minutes when the driving pressure was subsequently raised to the region of 15-25 psia following such a zero-flow condition. Similarly, when the driving pressure was returned to the operating range after having been set at 150 psia, substantially higher

* This simple relationship is correct where no liquid-wall interaction occurs (i.e., no wetting) as is nearly the case with mercury on a molybdenum surface.

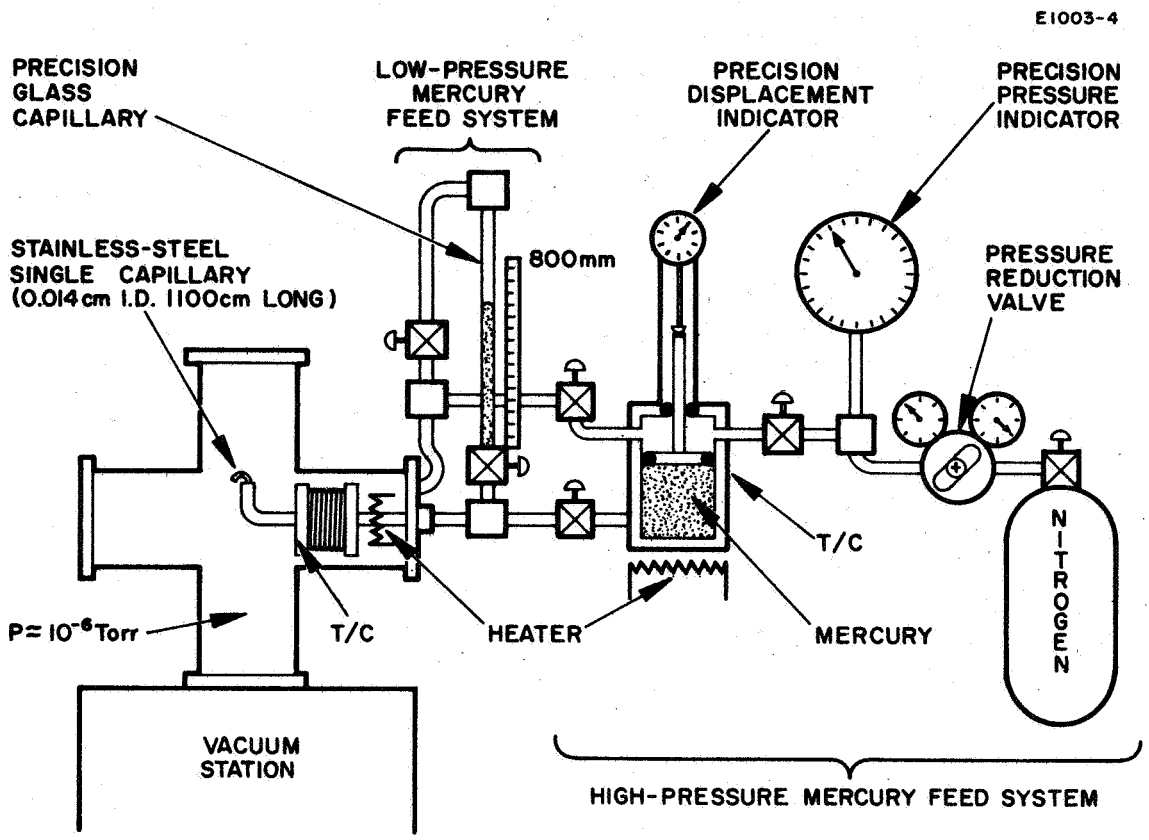

Fig. 9. Single-capillary-flow research apparatus (T/C = thermocouple).

(+ 20%) flow rates were recorded for as long as 30 minutes thereafter.

To gain better insight into the mechanisms involved in this anomalous behavior, a new flow system has been assembled which will permit testing of single-capillary mercury flow impedances under well-controlled vacuum and temperature conditions. In this setup (see Fig. 9) mercury is held in a piston-driven positive-displacement feed system from which it can either be driven directly through the flow impedance at pressures from 14.7 to 300 psia, or this system can be used only as a reservoir to deliver mercury to a precision-bore glass capillary serving as a manometer. Mercury from the manometer can then be used under the pressure of the mercury head alone for measurements in the range of 0 - 15.5 psia. At the higher driving pressures, the rate of displacement of the piston permits the measurement of the mercury flowrate, while the rate of displacement of the mercury meniscus in the glass capillary indicates the mercury flowrate at the lower pressures. The O-ring seals of the piston-driven feed system were lubricated with Apiezon-H vacuum grease which permits the mercury contained in the piston-driven feed system to be outgassed - under vacuum - at temperatures up to 150°C. For the measurements at lower driving pressures (where outgassing may be more critical) the mercury contained in the manometer can be outgassed - under vacuum - at even higher temperatures.

For the first tests with this setup a new single-capillary flow impedance has been prepared (denoted as SC-3) which consists of a 1,060-cm length of 0.014-cm i.d. type 304 stainless steel tubing. The interior of this capillary was chemically cleaned in the sequence of operations described below:

1. Washed in acetone
2. Washed in detergent and water
3. Etched in a mixture of equal parts HF, HNO_3, and H_2O
4. Washed in deionized water
5. Washed in acetone.

For some time the acid solution of step No. 3 discharged from the capillary carrying a black suspension of contaminants which were apparently lodged within the tube. After about 1 hour the discharge was clear. The chemical etch was continued for another 1/2 hour after that.

This capillary tube was next wound about a 10-cm diameter mandrel. On this mandrel, the capillary can be placed in vacuum (as shown in Fig. 9) where it can be heated to 250°C in order to drive out trapped gasses or vapors prior to operation with mercury.

At the writing of this report, the flow system and impedance have been assembled and the high-pressure feed system is filled with mercury. Both the stainless steel single capillary and the high-pressure feed system are presently being baked in a vacuum of 2×10^{-6} Torr.

B. High-Voltage Hydrogen-Bubble Isolator

A liquid-mercury high-voltage isolator was developed recently[14] at HRL under NASA Contract NAS 7-100 (Task Order #RD-26). In this device, shown in Fig. 10, a hydrogen bubble is injected into an electrically insulating teflon tube through which mercury flows. After the bubble has travelled a prescribed distance down the teflon tube, an electrical signal is generated by an electronic circuit connected with a bubble-sensing coil, and a new bubble is injected. The first bubble then proceeds to a porous-tungsten hydrogen vent, where it diffuses out of the feed line into the surrounding vacuum. Since at least one hydrogen bubble is present in the teflon tube at all times, this device serves to interrupt the electrical continuity through the mercury stream from one end of the insulating tube to the other.

To demonstrate their mutual compatibility, the hydrogen-bubble high-voltage isolator was operated in conjunction with an LM cathode. The hydrogen-bubble, high-voltage isolator was joined to the circular LM cathode with a single-capillary flow impedance. LM cathode discharge operation under the condition of high-voltage isolation was demonstrated for periods of several hours of uninterrupted automatic operation at voltages up to 4.5 kV, which was the maximum output voltage of the power supply available to this experiment. The maximum design voltage of the isolator is 5 kV.

The LM cathode functioned normally when operated in conjunction with the hydrogen-bubble isolator. Since the mercury flow impedance is located downstream of the isolator, the mercury driving pressure at the cathode remains substantially constant in spite of the alternate injection and evacuation of hydrogen bubbles from the flow line. No fluctuations were observed in the flow of mercury to the cathode in response to hydrogen bubble formation or evacuation at the isolator. The single-capillary flow impedance is sufficiently conductive to pass adequate mercury flow rates without imposing excessive pressures on the isolator.

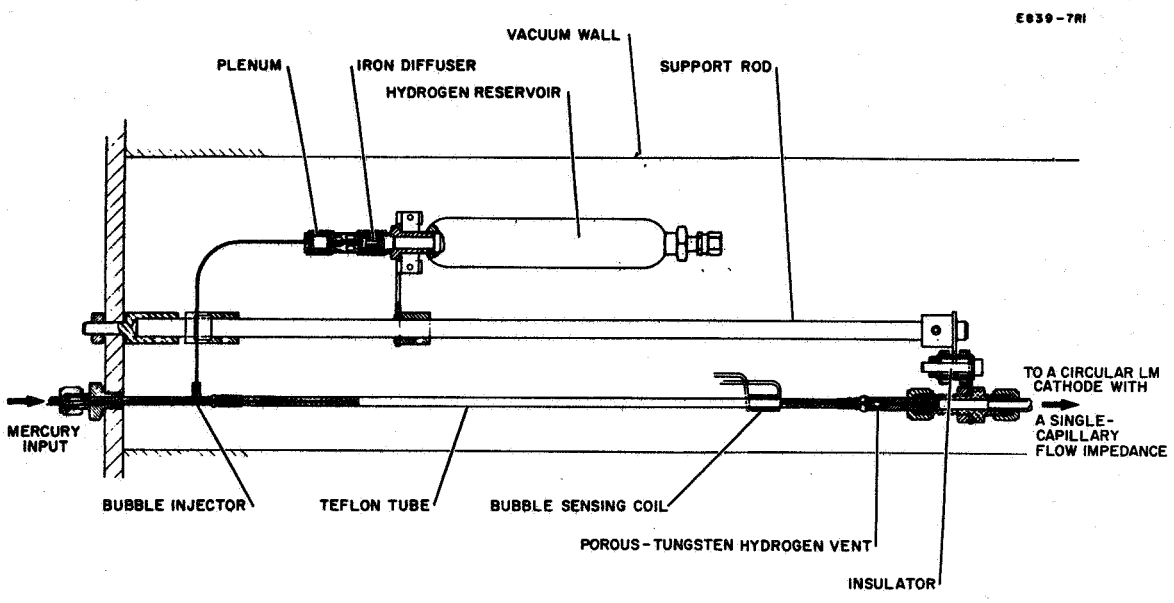

Fig. 10. High-voltage hydrogen-bubble isolator system.

PRECEDING PAGE BLANK NOT FILMED.

VI. CONCLUSIONS

A program is under way to optimize the electron-bombardment thruster for operation with an LM cathode. Discharge chamber losses in an existing 20-cm thruster have been reduced significantly by modifications of the baffle configuration and of the magnetic field geometry. The feasibility of efficient thruster operation both with a high-temperature LM cathode and with a high-perveance ion-extraction system at low specific impulse have been demonstrated with this thruster. The final stages of optimization and a demonstration of LM cathode thermal integration are to be realized with a 30-cm thruster which is now being assembled.

Accomplishments to date include:

1. A 30-cm bar-electromagnet thruster has been fabricated which attempts to exploit the experience gained through recent development of optimized thrusters at HRL, JPL, and LeRC. This thruster incorporates features necessary for thermal integration of the cathode within the overall thruster system and is estimated to weigh approximately 6.2 kg. The thruster is presently being assembled.

2. A modified 20-cm bar-electromagnet thruster has been operated with the following performance:

Beam Current	I_B = 550 mA
Source Energy per Ion*	V_S = 250 eV/ion
Mass Utilization	η_m = 85%
Specific Impulse	$I_{sp,\,eff}$ = 6,600 sec.

3. A new technique has been introduced for the assembly of LM cathodes which employs the use of shims to establish the uniformly small feed channels desired for high-temperature operation. This technique has been applied to the fabrication of an annular LM cathode and to a linear-slit LM cathode.

4. A circular LM cathode which is fed by a single-capillary flow impedance and the linear-slit cathode have both been operated satisfactorily in a diode discharge.

5. Annular cathode K-25-V has been operated at high temperature both in a diode discharge and in a 20-cm diameter electron-bombardment thruster. Thruster performance was close to the best previously obtained and the quantity

---

* V_S is the total energy required to form an ion, since no heater, vaporizer, or keeper power is required with the LM cathode.

of heat delivered by the discharge to the thruster was sufficiently small to permit its radiant dissipation from the thruster shell.

6. Discharge-chamber performance of the 20-cm thruster at $\eta_m = 80\%$ was found to deteriorate by as much as 100 eV/ion at a beam voltage of 3 kV when compared with the performance observed at 6 kV. Reoptimization at 3 kV or at lower voltages appears feasible.

7. An LM cathode neutralizer has been operated (under laboratory conditions) at $K_e/K_a \approx 200$ with a current of 1.9 A and a diode discharge voltage of ≤ 30 V. Operation at $K_e/K_a = 50$ appears attainable for operation in conjunction with a thruster.

8. Using a liquid-mercury high-voltage isolator, satisfactory LM cathode discharge operation was demonstrated under conditions of high-voltage isolation for periods of several hours of uninterrupted automatic operation at voltages up to 4.5 kV.

9. Measurements of Poiseuille flow of mercury through a single-capillary flow impedance were linear and repeatable to within the experimental error of $\pm$ 5% over the range from 1 to 5 A_{equiv}.

VII. RECOMMENDATIONS AND FUTURE PLANS

Continuation of the program during the next quarter is planned along the following lines:

- Initial testing of the 30-cm thruster. This effort will be supported, where applicable, by continuing optimization of the 20-cm thruster.
- Performance mapping of the 20-cm thruster.
- Continuation of measurements related to Poiseuille flow through single capillary tubes with the aim of developing techniques for accurate, instantaneous flow measurement and control in the range of interest for electrical propulsion.
- Performance mapping of annular cathode K-25-V; measurement of variations in the specific thermal loading $V_{K,th}$ as a function of cathode body temperature T_K and the electron-to-atom ratio K_e/K_a.
- Design of a new high-temperature cathode - either annular or linear-slit - for ultimate use with the 30-cm thruster.
- LM cathode neutralizer research and development.

PRECEDING PAGE BLANK NOT FILMED.

VIII. NEW TECHNOLOGY

During this reporting period, two items of new technology have been developed.

1. Linear-Slit LM Cathode
   Innovator: W. O. Eckhardt
   Progress Reports: First Quarterly Report of this Contract, 15 May 1968, pp. 18 & 19, and this report.

2. 30-cm Thermally-Integrated Electron-Bombardment Thruster Using an LM Cathode.
   Innovator: J. Hyman, Jr.
   Progress Reports: First Quarterly Report of this Contract, 15 May 1968, pp. 35-37, and this report.

PRECEDING PAGE BLANK NOT FILMED.

IX. REFERENCES

1. R. T. Bechtel, "Discharge Chamber Optimization of the SERT II Thruster," AIAA Paper No. 67-668.

2. R. T. Bechtel, G. A. Csiky, and D. C. Byers, "Performance of a 15-cm Diameter, Hollow-Cathode Kaufman Thruster," NASA TM X-52376.

3. W. R. Kerslake, D. C. Byers, and J. F. Staggs, "SERT II Experimental Thruster System," AIAA Paper No. 67-700.

4. J. Hyman, Jr., W. O. Eckhardt, J. W. Pfeifer, and J. A. Snyder, "High-Temperature LM Cathode Ion Thrusters," Quarterly Report No. 1, Contract JPL 952131, HRL 15 May 1968.

5. T. D. Masek and E. V. Pawlik, "Thrust System Technology for Solar Electric Propulsion," AIAA Paper No. 68-541, AIAA 4th Propulsion Joint Specialists Conference, Cleveland, Ohio, June 10-14, 1968.

6. E. A. Richley and W. R. Kerslake, "Bombardment Thruster Investigations at the Lewis Research Center", AIAA Paper No. 68-562, AIAA 4th Joint Specialists Conference, Cleveland, Ohio.

7. W. O. Eckhardt, K. W. Arnold, G. Hagen, J. Hyman, Jr., J. A. Snyder, and R. C. Knechtli, "High-Temperature Liquid-Mercury Cathodes for Ion Thrusters," Summary Report Contract No. NASW-1404, July 1967.

8. N. B. Kramer and H. J. King, "Extraction of Dense Ion Beams from Plasmas,", J. Appl. Phys. 38, 4019 (1967).

9. J. Hyman, W. O. Eckhardt, R. C. Knechtli, and C. R. Buckey, "Formation of Ion Beams from Plasma Sources: Part I," AIAA J. 2, 1739 (1964).

10. G. R. Brewer, K. Amboss, G. Nudd, H. J. King, R. Seliger and S. Kami, "Ion Engine Thrust Vector Study," JPL Contract 952129, Monthly Progress Report No. 4.

11. Private Communication with Paul D. Reader of JPL, 1968.

12. W. O. Eckhardt, H. J. King, J. A. Snyder, J. W. Ward, W. D. Myers, and R. C. Knechtli, "Liquid-Mercury Cathode Electron-Bombardment Ion Thrusters," Summary Report Contract No. NAS 3-6262, Oct. 1966.

13. "Solar Powered Electric Propulsion Spacecraft Study," Final Report, JPL Contract No. 951144, Hughes Space Systems Division, December 1965.

14. J. H. Molitor, H. J. King, and S. Kami, "A Study of Liquid Mercury Isolator Development," Sept. 1967, Final Report, Contract No. NAS 7-539.